6794 *Biochemistry* **2009,** *48,* 6794–6804
DOI: 10.1021/bi9007484

BIOCHEMISTRY
including biophysical chemistry & molecular biology
Article

Charge Conduction Properties of a Parallel-Stranded DNA G-Quadruplex: Implications for Chromosomal Oxidative Damage†

Yu Chuan Huang,‡ Alan K. H. Cheng,§ Hua-Zhong Yu,§ and Dipankar Sen*,‡,§

‡*Department of Molecular Biology and Biochemistry and* §*Department of Chemistry, Simon Fraser University, Burnaby, British Columbia V5A 1S6, Canada*

Received April 30, 2009; Revised Manuscript Received June 12, 2009

ABSTRACT: The charge-flow properties and concomitant guanine damage patterns of a number of intermolecular and wholly parallel-stranded DNA G-quadruplexes were investigated. The DNA constructs were structurally well-defined and consisted of the G-quadruplex sandwiched and stacked between two Watson−Crick base-paired duplexes. Such duplex−quadruplex−duplex constructs were designed to minimize torsional stress as well as steric crowding at the duplex−quadruplex junctions. When anthraquinone was used to induce charge flow within the constructs, it was found that the quadruplex served both as a sink and as a moderately good conductor of electron holes, relative to DNA duplexes. Most strikingly, the quadruplex suffered very little charge-flow generated oxidative damage relative to guanines in the duplex regions and, indeed, to guanines in antiparallel quadruplexes reported in prior studies. It is likely that these differences result from a combination of steric and electronic factors. A biological conclusion that may be drawn from these data is that if, as anticipated, G-quadruplex structures form *in vivo* at the telomeres and other loci in eukaryotic chromosomes, their ability to serve as protective sinks against chromosomal oxidative damage may depend on their specific character and topology. From a separate perspective, our results on the conduction properties of duplex−quadruplex−duplex DNA composites suggest the utility of G-quadruplexes as junction modules in the construction of DNA-based biosensors and nanocircuitry.

The linear nuclear chromosomes of higher (eukaryotic) organisms terminate in telomeres, which are repetitive DNA sequences with an asymmetric distribution of bases in the two strands (typically guanine- and thymine-enriched in one strand and adenine and cytosine in the other) (*1*, *2*). Watson, in 1972, coined the "end replication problem" which describes the intrinsic inability of DNA polymerases to completely replicate the ends of chromosomes owing to problems of primer placement on the lagging strand of replication (*3*). Nature solves this problem with telomerase, a specialized reverse transcriptase enzyme, which extends the telomeric repeat so as to prevent the loss of chromosomal information (*4*). When telomeres become too short, their remnants unfold from their compact structure into an "uncapped" form (*5*). Normal cells recognize this and either undergo cellular senescence or apoptosis (*6*). It is generally accepted that these two mechanisms are methods by which the cell prevents itself from becoming cancerous (*4*); thus, understanding the structure and mechanism of action of telomeres is pertinent for a deeper insight into cancer as well as into overall genomic stability.

The extreme end of the 3′ (guanine- and thymine-rich) strand of a telomere in living cells has been found to be single stranded (*1*). It has been known for some time that guanine-rich single-stranded DNAs *in vitro* are able to form, under physiological salt concentrations, a family of nonlinear and highly ordered folded structures termed guanine or G-quadruplexes (*1*, *2*). In G-quadruplexes, guanine residues from four different DNA strands or from different regions of one or two strands hydrogen bond to each other via Hoogsteen base pairing to form guanine quartets (*7*−*9*). The overall topology of G-quadruplexes can be immensely varied, but among the most stable and structurally well-defined are parallel quadruplexes in which all participating strands lie in a parallel orientation. Such parallel quadruplexes, conveniently formed using four distinct G-rich strands of DNA, are termed G4 DNA structures (*7*, *10*, *11*). K^+ and Na^+ ions are found to support G-quadruplex formation, and these cations have been shown to coordinate to and stabilize two adjacent quartets; by contrast, Li^+ ions inhibit quadruplex assembly (*7*, *10*). Because telomeric sequences readily form G-quadruplexes *in vitro*, it has been proposed that they also likely form quadruplexes *in vivo* (*7*−*9*). Owing to the inseparable association between telomeres and aging/cancer, it has also been proposed that G-rich regions of genomes, and G-quadruplexes, may serve as oxidizable sinks to protect the genome from

†This work was funded by the Natural Sciences and Engineering Research Council (NSERC, Grant RGPIN/105785) and by the Canadian Institute for Advanced Research (CIFAR). A.K.H.C. is grateful to NSERC, Simon Fraser University, and the Provincial Government of British Columbia for postgraduate scholarships. D.S. is an Associate of the Canadian Institute for Advanced Research (CIFAR).

*Corresponding author. E-mail: sen@sfu.ca. Phone: (778) 782-4386. Fax: (778) 782-5583.

 Published on Web 06/17/2009

oxidative damage and so confer genome stability (*12*−*15*). This theory is based on observations that DNA helices are able to conduct charge along their lengths (*16*).

Charge transfer through double-stranded DNA (dsDNA)[1] was first proposed over 40 years ago (*16*). Intensive research in recent years has demonstrated that DNA double helices in aqueous solution do conduct electrical charge (reviewed recently in refs *12* and (*17*−*19*)). Two kinds of charge carriers have been characterized in DNA double helices: (a) nucleobase radical cations ("electron holes") and (b) radical anions ("excess electrons"). Hole transfer has been studied in much greater detail and can be initiated photochemically by excitation of a sensitizer such as anthraquinone (AQ), which is covalently attached and end-stacked upon a double helix. Of the DNA bases guanine (G) is the most easily oxidized, and G radical cations ($G^{+\bullet}$) can migrate over significant distances (> 200 Å) along the length of a helix (*12*, *20*, *21*). Both charge hopping and superexchange are thought to operate at different distance scales (*22*−*24*); recently, a refinement of the hopping model, the "phonon-assisted polaron-like hopping" model, has been used to describe long-range hole conduction (*20*, *21*). Such hole transport through DNA can be easily monitored using Maxam−Gilbert sequencing. Guanine radical cations are susceptible to a degree to reaction with water and with dissolved oxygen, to give guanine oxidation products such as 8-oxoguanine or diaminooxazalone (*25*). Incubation with hot piperidine is known to break the DNA strand at such sites (*25*). The resulting DNA fragments can be analyzed in denaturing polyacrylamide gels, with the observed level of charge-flow-generated DNA cleavage at a given site being proportional to the lifetime of the mobile radical cation upon that guanine (*26*).

While charge flow through guanine-rich DNA duplexes has been investigated thoroughly to date, indeed, has been coopted for the development of a growing technology of electrical biosensors (*27*−*29*), the charge transport properties of guanine quadruplexes has been investigated to a much more modest degree.

From an early study of charge transfer in G-quadruplexes using electrochemistry, Szalai and Thorp (2000) reported that the electrochemical behavior of $Ru(bpy)_3^{2+}$ (bpy = 2,2′-bipyridine) intercalated either in B-DNA or in a variety of antiparallel, intramolecular quadruplexes was different (*30*). They reported that electron transfer from guanine residues in quadruplexes was faster than from guanine residues in duplex DNA. Delaney and Barton (2003) used an intercalating rhodium photooxidant to compare charge-flow and oxidative damage patterns in the duplex and quadruplex components of a duplex−antiparallel quadruplex composite (the quadruplex was formed in intramolecular fashion by an single-stranded, human telomeric overhang off the duplex) (*31*). They noted that the quadruplex (in particular, certain guanines within the quadruplex) appeared to function as more effective hole traps (and suffered a higher level of oxidative damage) than a guanine doublet located in the duplex region. Later experiments by Ndlebe and Schuster (*32*) and Kawai et al. (*33*) also reported evidence that guanines within quartets were at least 50% more likely to be damaged compared to guanines in duplexes. In the study by Ndlebe and Schuster (*32*), G-rich hairpins were dimerized into quadruplexes such that the hairpin stems were either parallel or antiparallel to each other (in both situations, however, the strand orientations within the resulting quadruplexes would necessarily be wholly or partially antiparallel).

By contrast to the above, a study by Pothukuchy et al. (*34*) reported different conclusions. These authors studied photocleavage of duplex and quadruplex DNA by a trioxatriangulenium cation (TOTA). Overall, they reported lower levels of charge-flow-related base damage at guanine repeats within quadruplex DNA relative to such repeats in duplex DNA (*34*).

Two observations are pertinent to the above studies: first, they have been carried out on diverse G-quadruplexes of often incompletely characterized geometries and topologies. For instance, the precise fold or folds of the human telomeric repeat, such as studied by Delaney and Barton (*31*), continue to be contentious (*35*−*41*). Second, in a number of the above constructs there is uncertainty about whether their duplex and quadruplex components can comfortably stack or not, owing to both steric crowding (such as when two double helices, of 20 Å diameter each, are required to stack side by side upon one 26 Å quadruplex) and torsional stress at the duplex−quadruplex junctions. G-quadruplexes are a class of extremely polymorphic structures; therefore, the lack of unambiguous definition of quadruplex structure/topology and of quadruplex−duplex stacking interactions has prevented the formulation to date of a *general* statement about the ability of quadruplexes to (i) conduct electron holes, (ii) act as sinks for electron holes, and (iii) be oxidatively damaged in the process.

We therefore decided to study the best characterized as well as most stable form of the G-quadruplex, namely, an all-parallel-stranded quadruplex made up of four distinct strands of DNA (and therefore lacking any connecting loops between the strands).

As noted above, G-quadruplexes tend to be structurally polymorphic, whereby modest changes in solution conditions can give rise to architectures with different folds, topologies, and molecularity. However, of all quadruplexes, four-stranded, all-parallel structures containing five or more adjacent G-quartets enjoy very high thermodynamic as well as kinetic stabilities (*10*, *42*−*44*). A DNA oligomer of 35−40-nt length, containing a single block of five contiguous guanines (and no plausible self-folded Watson−Crick structures), is able to form *only* an intermolecular parallel quadruplex (*7*, *10*, *11*, *42*−*44*); no evidence for the formation of an intermolecular antiparallel quadruplex by such an oligomer has ever been reported. Therefore, the issue of polymorphism and uncertainty about the nature of the quadruplex fold are eliminated in the D-Q-D structures studied herein.

Our constructs were designed to have the quadruplex sandwiched between two duplex elements, such that the potential charge-flow path would be from an initiating (proximal) duplex to the quadruplex and into the distal duplex. To eliminate steric crowding at the duplex−quadruplex junctions, such as was likely found with many of the constructs used by prior investigators in their studies on antiparallel quadruplexes (*31*, *32*, *34*), the junctions in our constructs had a single duplex stacking upon a quadruplex. To minimize the expected helical strain as DNA strands transitioned between two different helical forms, each duplex−quadruplex junction incorporated a strand nick, which does not ordinarily interfere with charge flow (*45*) but should ensure optimal stacking between the two kinds of helices at each junction.

[1]Abbreviations: dsDNA, double-stranded DNA; PAGE, polyacrylamide gel electrophoresis; EDTA, ethylenediaminetetraacetic acid; TBE, Tris−borate−EDTA buffer; TE, Tris−EDTA buffer; N-NHS, *N*-hydroxysuccinimide; TEAA. triethylammonium acetate; CH_3CN, acetonitrile.

MATERIALS AND METHODS

DNA Purification and Preparation. Unmodified DNA oligonucleotides were purchased from Core DNA Services, Inc. (Calgary, Alberta, Canada) and size-purified using denaturing (50% urea, w/v) polyacrylamide gel electrophoresis (PAGE). Quantification was done on a Cary 300Bio UV−visible spectrophotometer (Varian Instruments) using an absorbance at 260 nm estimated for single-stranded DNA. 5′-Amino-modified DNA oligonucleotides were purchased from Core DNA Services, Inc., and were subjected to covalent coupling with anthraquinone (AQ) as described by Fahlman and Sen (*27*) and Huang et al. (*29*). Briefly, the covalent attachment was accomplished by reacting the *N*-hydroxysuccinimide (NHS) ester of anthraquinone-2-carboxylic acid with the amino-terminated DNA. AQ-DNA was purified by HPLC (Agilent Technologies) using an Agilent Zorbax ODS RP-18 5 μm column and eluted with a gradient of 0.05 M triethylammonium acetate (TEAA, pH = 8.0)/CH_3CN and 100% CH_3CN at 1.0 mL/min. To lower the background cleavage oligonucleotides used for the charge-flow experiments were end-labeled with ^{32}P (using standard kinasing procedures) and then PAGE purified following a pretreatment with 10% piperidine (v/v) at 90 °C for 30 min followed by lyophilization.

Preparation of DNA/Quadruplex Conjugates for AQ Charge Transfer. The four-stranded guanine quadruplex construct (termed LS_3) was assembled by coincubation of L (at 57 μM) and S (at 570 μM). Both L and S were first denatured in 100 mM LiOH in a boiling water bath for 3 min and then brought to pH 7.4 by addition of 100 mM HCl followed by Tris-HCl (pH = 7.4) for neutralization. The assemblies were then incubated with 10 mM KCl in a 50 °C water bath for 48 h. The resulting quadruplex products were run on a 15% nondenaturing polyacrylamide gel, in 90 mM TBE running buffer at 4 °C, to separate the LS_3 product from the other quadruplex complexes (L_4, L_3S, and L_2S_2). The LS_3 product was cut from the gel and eluted into 50 mM Tris-HCl, pH 7.4, and 100 mM KCl overnight, ethanol precipitated, and then stored dissolved in the same buffer at 4 °C prior to use. The final hybridized constructs (such as $LS_3 \cdot P \cdot D$) were assembled by mixing the appropriate quadruplexes and/or single strands in 50 mM Tris-HCl, pH 7.4, 100 mM KCl, and 1 mM $MgCl_2$.

Charge Transfer of DNA Duplex/Quadruplex Conjugates with AQ. The DNA constructs were first incubated at 4 °C for 1 h prior to photoirradiation to initiate charge flow. Irradiation at 365 nm was carried out at 4 °C in 50 mM Tris-HCl (pH = 7.4), 100 mM KCl, and 1 mM $MgCl_2$ (unless otherwise stated). The samples were placed under a UVP Black-Ray UVL-56 lamp (365 nm) for 1 h at a distance of 4 cm from the bulb. Temperature was maintained by placing the sample tubes in a water bath set to the desired temperature. Following irradiation, the samples were loaded in a 15% nondenaturing polyacrylamide gel run at 4 °C. The desired complexes (i.e., L·cL, $LS_3 \cdot P$, $LS_3 \cdot P \cdot D$, Gap5, or $L \cdot P \cdot D$) were cut from the gel and eluted into 10 mM Tris-HCl, pH 7.4, and 100 μM EDTA (TE buffer) overnight. The eluted DNA was ethanol precipitated using glycogen as a carrier. The DNA pellets were then dissolved and treated with 10% piperidine (v/v) at 90 °C for 30 min. All samples were analyzed in 12% denaturing polyacrylamide gels.

Chemical Protection Assays with DMS, $KMnO_4$, DEPC, and NH_2OH. Dimethyl sulfate (DMS), potassium permanganate ($KMnO_4$), and hydroxylamine (NH_2OH) protection assays were carried out following the standard protocols (*46*).

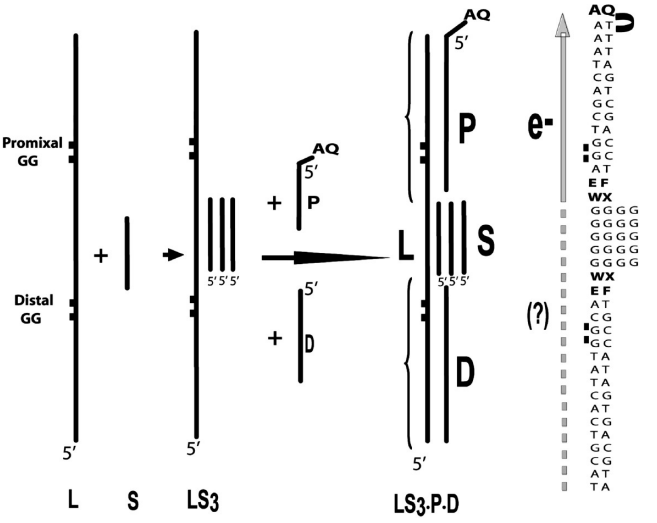

FIGURE 1: A schematic for the assembly of the duplex−quadruplex−duplex construct, $LS_3 \cdot P \cdot D$ (the symbol · signifies a Watson−Crick-type hybridization). Coincubation of 35-nt, G-rich DNA oligomers, L, with a short oligonucleotide, S (dG_5) in the presence of potassium choride generates a number of distinct intermolecular, parallel-stranded quadruplex products, of which the LS_3 product was purified and hybridized to short DNA oligonucleotides, P and D (P being derivatized at its 5′ terminus with an anthraquinone (AQ) moiety). The nucleotide sequence of the entire $LS_3 \cdot P \cdot D$ product is shown at the extreme right. Three variants of $LS_3 \cdot P \cdot D$ were tested, "TG_5T", "CG_5C", and "AG_5A", in which the bases "EW" were CT, GC, and GA, respectively. The base "F" was the Watson−Crick complement of "E" and "X" the complement of "W".

Upon the addition of their respective "stop" solutions, the samples were ethanol precipitated to recover the DNA and treated with 10% (v/v) piperidine at 90 °C for 30 min, dried, and electrophoresed through a 12% denaturing polyacrylamide gel.

Data Analysis. Imaging and densitometry of sequencing gels were carried out using a Typhoon 9410 phosphorimager and quantitated with ImageQuant 5.2 (Amersham Bioscience). In all situations, guanine damage levels in DNA samples containing anthraquinone-labeled (charge-flow-enabled) assemblages were corrected for nonspecific cleavage at those same guanines in no anthraquinone (charge-flow-disabled) control samples. The densitometric ratio of the distal doublets to the proximal doublets (GGd/GGp) describing the efficiency of charge transfer was calculated by the net percentage cleavage of distal damage divided by the net percentage cleavage of proximal damage.

RESULTS

Design of Constructs for Biochemical Assays. Figure 1 shows a schematic for the assembly of a $LS_3 \cdot P \cdot D$ duplex−quadruplex−duplex (D-Q-D) construct. Three similar 36-nt DNA oligonucleotides, L (in which the base sequence "EW" in Figure 1 refers to CT, GC, and GA, respectively), were designed on the basis of prior DNA sequences that had been shown to be good conductors of charge (within the structural context of DNA duplexes). Analysis of the sequence of the three L sequences using the Mfold RNA/DNA folding program indicated that none of them folded to any stable secondary structure. The sequence of L incorporated a central G_5 motif (required for quadruplex formation) as well as flanking sequences that would form the sandwiching duplexes. Each flanking sequence incorporated a GG sequence (termed the "proximal" and "distal" GG, defined

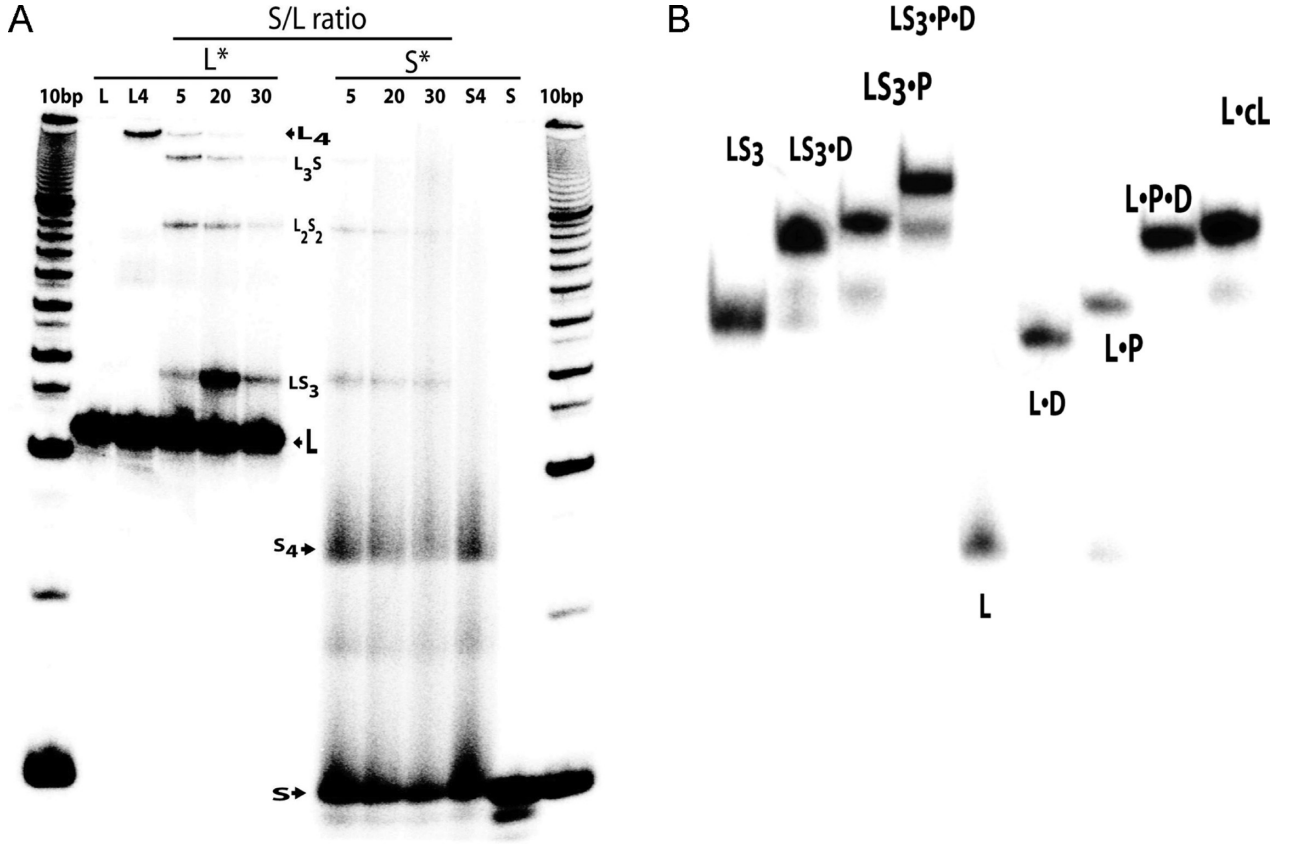

FIGURE 2: (A) A nondenaturing polyacrylamide gel that shows the results of coincubation of the DNA oligomers L and S (here, the L is "TG_5T"), at different stoichiometric ratios, in the presence of potassium chloride. L* and S* indicate respectively mixtures in which radiolabeled L was incubated with unlabeled S, and vice versa. The lanes marked "5", "20", and "30" refer to the molar ratios of S:L in those incubations. (B) A native polyacrylamide gel showing the stepwise assembly of different DNA constructs. Left: $LS_3 \cdot P \cdot D$ was assembled from purified, radiolabeled LS_3 and unlabeled P and S oligomers. Right: The stepwise assembly of the $L \cdot P \cdot D$ and $L \cdot cL$ complexes.

in relation to the anthraquinone moiety in the final $LS_3 \cdot P \cdot D$ assemblage) for convenient monitoring of guanine damage at fixed duplex sites. Coincubation of an L oligonucleotide with a shorter DNA oligmer, S (whose sequence was simply dG_5), in the presence of potassium would be expected to generate a series of G-quadruplexes made up of different stochiometries of L and S (L_4, L_3S, L_2S_2, LS_3, and S_4, respectively) (*10*). The quadruplex product LS_3 could then be identified, purified, and hybridized with two short DNA oligonucleotides (D and P, 17 and 14 nts, respectively) complementary to the two sequence elements flanking the central G_5 of an L oligonucleotide (P has an anthraquione residue covalently attached to its 5′-terminal phosphate, separated from the phosphate by six methylene units). In the final $LS_3 \cdot P \cdot D$ so assembled (where · signifies Watson−Crick-type hybridization), the anthraquinone would stack atop the P helix (*19*) and so set up a procedure for UV irradiation-mediated charge flow through that helix and through the $LS_3 \cdot P \cdot D$ construct as a whole. The full nucleotide sequence of the $LS_3 \cdot P \cdot D$ composites is shown at the extreme right of Figure 1. The two strand discontinuities between the quadruplex and its two flanking duplex elements (the overall assemblage nevertheless maintains a continuum of base pairing, with every nucleotide of L involved in base pairing in a duplex or quadruplex within $LS_3 \cdot P \cdot D$) were incorporated to minimize torsional stress at the duplex−quadruplex junctions and so to enable optimal stacking between the terminal base pairs and base quartets of those distinct kinds of helices.

Figure 2A shows a nondenaturing gel in which the formation of the different quadruplex products from the L and S oligonucleotides is highlighted (here, the L oligonucleotide is "TG_5T", the identity of whose variable base sequence, "EW", as shown in Figure 1, is CT). The individual L and S oligonucleotides were first denatured at 100 °C for 3 min in 100 mM LiOH to disrupt any preformed quadruplex structures, pH neutralized, and mixed together in different stoichiometries in TE buffer (10 mM Tris-HCl, pH 8.0, 0.1 mM EDTA). The solutions were then made up to 10 mM KCl in TE buffer and allowed to remain at 50 °C for 48 h. Parallel experiments were performed, using both ^{32}P-labeled L with unlabeled S and ^{32}P-labeled S with unlabeled L, in order to enable unambiguous identification of the different quadruplex products (*10*), as shown in Figure 2A. By varying the ratios of S to L, we were able to optimize the formation of the quadruplex product of interest, LS_3, which was then eluted from the gel into 50 mM Tris-HCl, pH 7.4, and 100 mM KCl. The purified quadruplex was stored in this buffer at 4 °C until used for hybridization. Under these conditions LS_3 was found to be stable and did not dissociate to L and S (for instance, just one band, corresponding to the expected LS_3 mobility, was observed in lane 1 of Figure 2B, indicating its stability).

Figure 2B shows a nondenaturing gel (containing potassium) detailing the step-by-step assembly of the complete $LS_3 \cdot P \cdot D$ product, as well as of two other products to be used as controls for the charge-flow experiments ($L \cdot P \cdot D$ and $L \cdot cL$, where cL is a 36-nt oligonucleotide wholly complementary to L). All of these products, when gel-purified into TE + 100 mM KCl and rerun in a nondenaturing gel run at 4 °C, were found to maintain their structural integrity. Figure 3 schematizes the various DNA

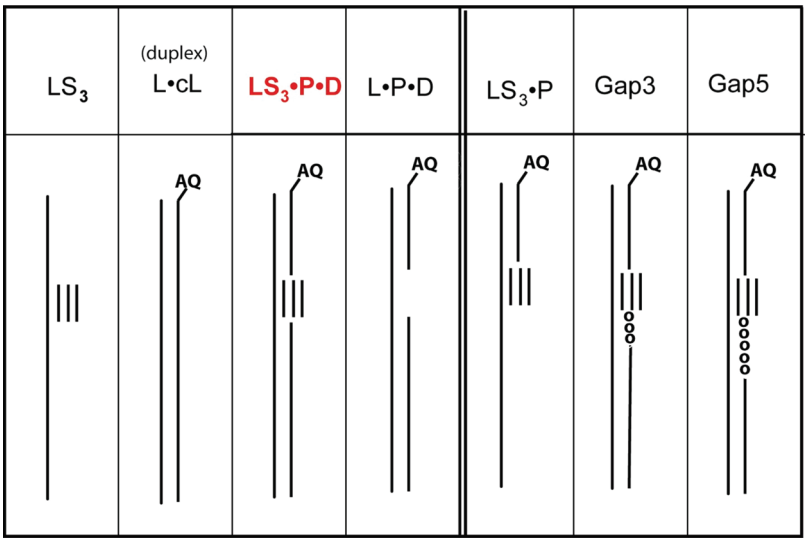

FIGURE 3: Schematic drawings of the different DNA constructs studied for their ability to conduct electron holes. L·cL is a purely Watson−Crick duplex of L and its complementary strand, cL. LS_3·P·D is the duplex−quadruplex−duplex that is the object of this study. The "Gap3" and "Gap5" constructs refer to LS_3·P·D-like assemblies that differ from LS_3·P·D in that the D oligomer within them has been replaced by truncated versions of D, which are shorter at their 5′ end by 3 and 5 nts than full-sized D. This results in the Gap3 and Gap5 constructs having short single-stranded stretches of 3 and 5nt, respectively, separating the duplex and the quadruplex at the distal junction.

constructs that were assembled as controls and comparison points for LS_3·P·D: LS_3·P, Gap3 and Gap5 (the last two incorporating gaps of 3 and 5 nt, respectively, between the quadruplex and the distal duplex), L·P·D, and L·cL. Overall, the design of these constructs permitted the probing of charge transfer (and its oxidative consequences) in three distinct regions of L: at the proximal guanine doublet, at the five quadruplex guanines, and at the distal guanine doublet.

Confirmation of the Integrity of Quadruplex Constructs Using Chemical Protection. The structural integrity of the LS_3·P·D construct, as well as of the various control constructs, was probed using chemical protection assays. Figure 4A shows data that confirm the successful formation of L·cL, LS_3, LS_3·P·D, and L·P·D (in these constructs L is "TG_5T", as defined earlier. Constructions using the other L oligonucleotides gave very similar results). Dimethyl sulfate (DMS, used in the "G" lanes) was used to test the formation of the Hoogsteen-bonded architecture of G-quadruplexes. In those constructs where quadruplexes were expected to form (LS_3 and LS_3·P·D), full protection from DMS methylation of the five central guanines was observed, as expected (*7*, *10*). In the other constructs (L, L·P·D, and L·cL), high levels of methylation were observed at these five guanines, indicative of their noninvolvement in quadruplex formation. Significant methylation was also seen at both the distal and proximal GG motifs in all constructs; this was expected since these guanines were located in single-stranded regions (in L and LS_3) or in duplexes (in L·P·D, L·cL, and LS_3·P·D), in both of which the N7 methylation site of guanines is accessible to the solvent and to DMS (*36*). Protection assays with potassium permanganate ($KMnO_4$) and hydroxylamine (NH_2OH) (for the "T" and "C" lanes, respectively) were used to verify the formation of duplex regions, on the basis of the exclusive reaction of these chemicals with single-stranded/unstacked thymines and cytosines, respectively (*43*). Using the L·cL and L lanes for comparison, it is clear that the LS_3 construct was not protected from either $KMnO_4$ or NH_2OH modification, confirming the presence of single-stranded arms within it. However, both LS_3·P·D and L·P·D were fully protected from NH_2OH modification. $KMnO_4$ protection assays of LS_3·P·D and L·P·D verified the existence of duplex regions flanking the quadruplex region but showed very slight modification of the two duplex thymines immediately flanking the quadruplex, on both its 5′ and 3′ ends (shown with arrows in Figure 4A). This slight reactivity is not unexpected, since some fraying of the ends of the duplexes may occur. In addition, the location of these bases at sites of change in the DNA architecture (from duplex to quadruplex in LS_3·P·D and duplex to single strand in L·P·D) may be pertinent.

Panels B and C of Figure 4 show analogous gels for the other two LS_3·P·D constructions, in which the constructs are made respectively from the "CG_5C" and "AG_5A" L oligonucleotides and their appropriate complements. The chemical protection features of constructs made from "CG_5C" (Figure 4B) closely match those made with "TG_5T" (Figure 4A). The constructs made from "AG_5A" (Figure 4C) also resemble the other two, with the notable difference that while in this case the junction adenines on either side of the quadruplex in L·P·D are reactive to diethyl pyrocarbonate (DEPC), those in LS_3·P·D are not. This either may be due to less fraying of the duplex ends within this LS_3·P·D construct or reflect a property of the modifying chemical, DEPC, to the specifics of the unstacked adenines and guanines that it typically reacts with.

Although chemical probing of this kind provides a relatively crude assessment of the structure and, particularly, the dynamics of helix junctions, the above results help to confirm that the L·cL, LS_3, L·P·D, and LS_3·P·D constructs are indeed what they were intended to be and respond to chemical probing in ways they were expected to.

Charge-Flow Patterns through D-Q-D Constructs. Figure 5A compares DNA strand-cleavage patterns at guanines as a result of charge flow through two kinds of DNA constructs: the perfect Watson−Crick duplex, L·cL, and the LS_3·P·D D-Q-D construct. The "N" lanes show DNA complexes that do not incorporate an AQ-derivatized L oligonucleotide; the two "AQ" lanes show the results of either one (for L·cL) or two independent experiments (for LS_3·P·D) on complexes that do incorporate

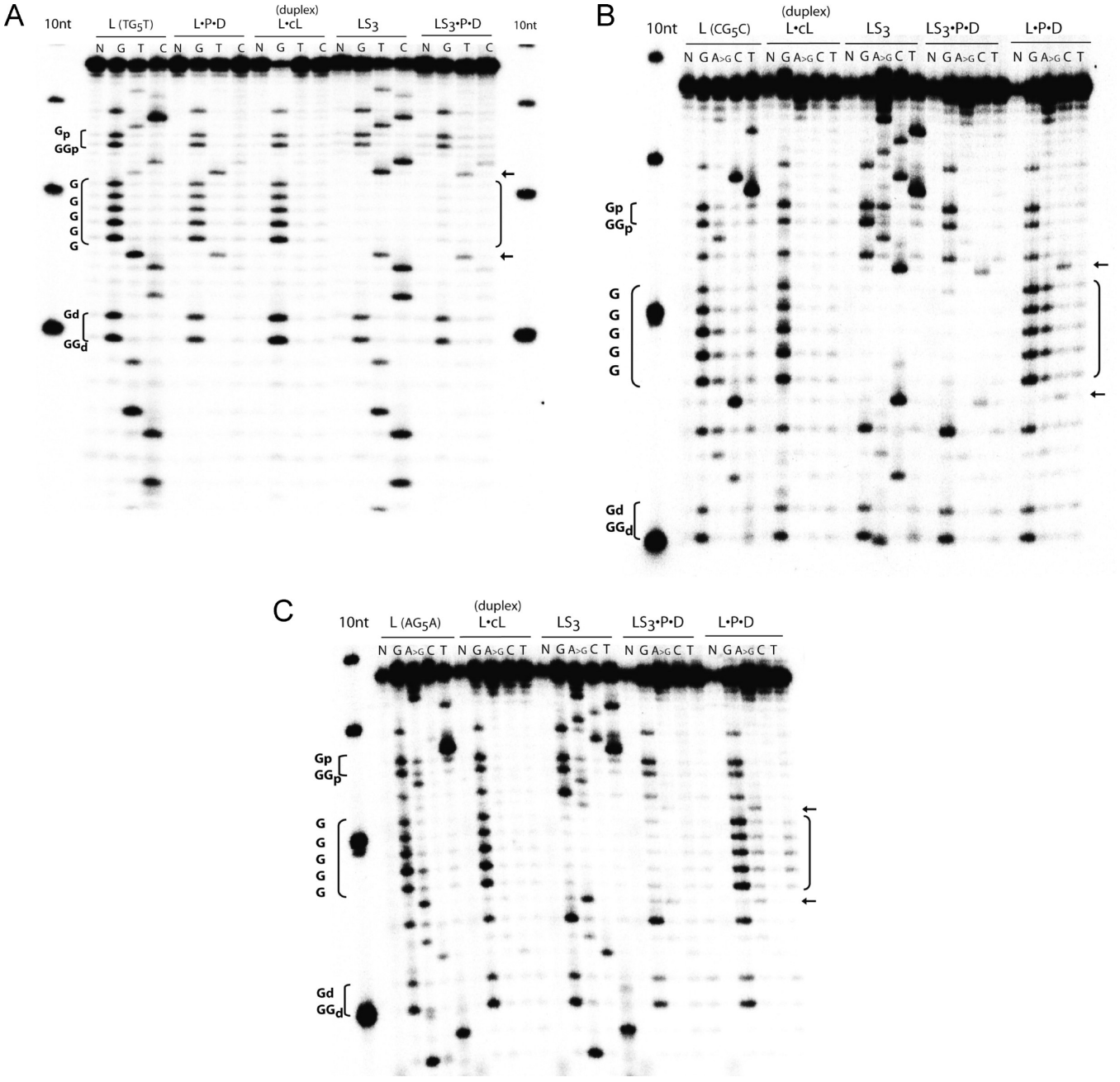

FIGURE 4: Chemical protection assays of DNA complexes formed by three different L oligonucleotides: "TG_5T" (panel A), "CG_5C" (panel B), and "AG_5A" (panel C). The lanes "N" refer to samples not subjected to any chemical treatment; "G" lanes have been treated with dimethyl sulfate (DMS), "T" with potassium permanganate ($KMnO_4$), "C" with hydroxylamine (NH_2OH), and "A > G" with diethyl pyrocarbonate (DEPC). The proximal G-doublet (Gp, GGp), distal doublet (Gd, GGd), and the five central guanines for quadruplex formation (GGGGG) are shown. The arrows to the right show the positions of the bases immediately flanking the five central guanines within L (the bases that correspond to "W" in Figure 1).

AQ-derivatized L oligonucleotides (enabling charge flow). All DNA complexes, whether in the "N" or the "AQ" lanes, were subjected identically to light irradiation and to subsequent treatment with hot piperidine.

The first observation is that all three L·cL duplexes conduct significant charge, as evidenced by guanine damage within them across their lengths, including at the proximal and distal guanine doublets as well as at the central five guanines. In both the proximal and distal doublets, damage is heavily localized in the 5′-most of the two guanines, a pattern characteristic of hole transfer in DNA (*26*). Damage is also greatest at the 5′-most of the central five guanines (and least in the 3′-most guanine). Under our experimental conditions the presence or absence of a nick in the duplex did not make any difference to the duplex's charge conduction properties; we have consistently found this to be so for DNA duplexes (*45*).

By contrast, three important observations can be made about the conductivity of the three $LS_3 \cdot P \cdot D$ constructs: (a) in all cases the overall levels of guanine damage are lower than in their analogous duplexes; (b) in all three $LS_3 \cdot P \cdot D$ constructs guanine damage resulting from charge flow can be seen in *both* duplex elements, proximal and distal from the anthraquinone; and (c) with the single exception of significant damage at the 5′-most guanine of the quadruplex-forming G_5 stretch, the quadruplex guanines remain essentially undamaged by the charge flow. This last observation, in particular, stands in dramatic contrast

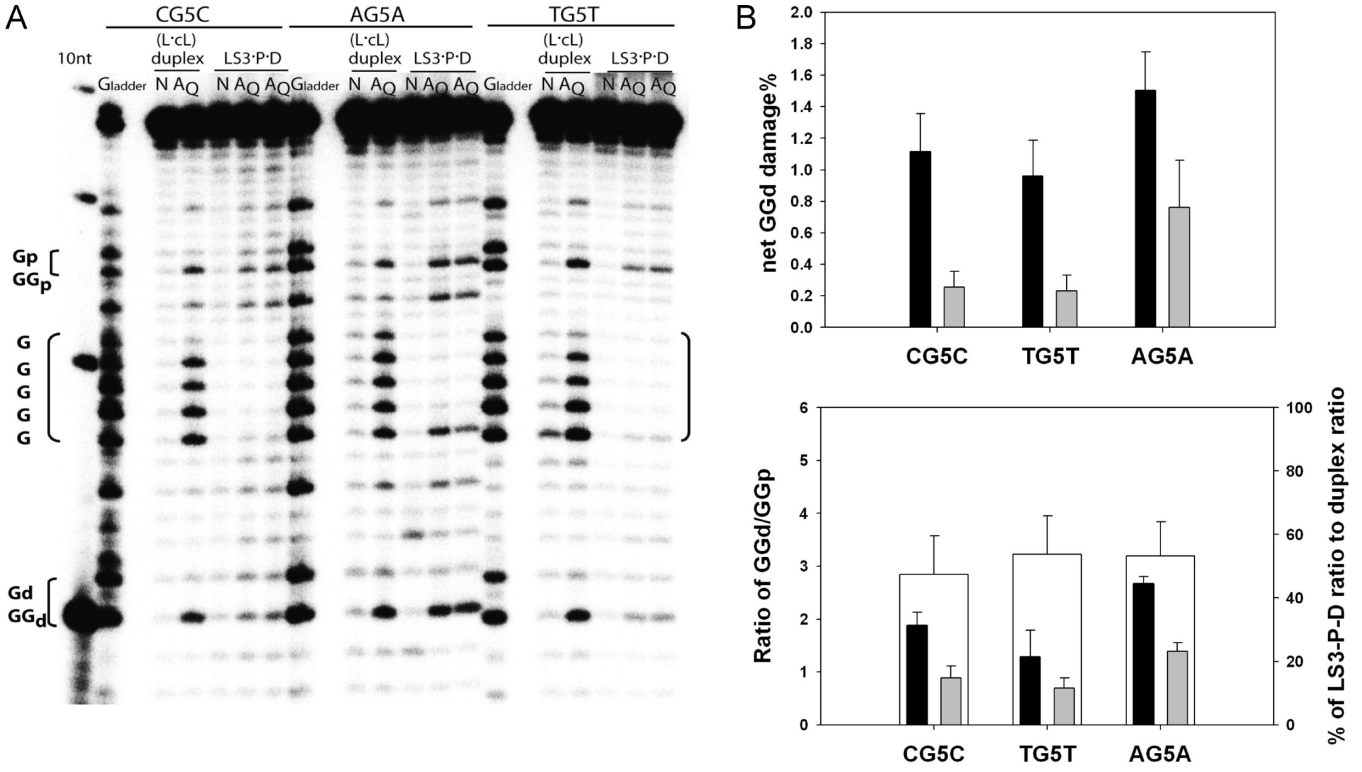

FIGURE 5: (A) Charge-flow-generated guanine damage/DNA cleavage patterns in the duplex L·cL and in the $LS_3 \cdot P \cdot D$ complex, assembled in each case from the "CG_5C", "AG_5A", and "TG_5T" variants of L (and the appropriately complementary oligonucleotides). The proximal and distal guanine doublets and the quadruplex-forming GGGGG motif are indicated, as in Figure 4. The "N" lanes show DNA complexes that do not incorporate an AQ-derivatized L oligonucletide; the two "AQ" lanes show two independent experiments on complexes containing AQ-derivatized L oligonucleotides. All DNA complexes in the "N" and "AQ" lanes were subjected comparably to light irradiation. (B) Upper: A histogram showing levels of charge-flow-related DNA cleavage at the 5′-most distal guanine (GGd in panel A) of the three L·cL duplexes (black bars) and the three $LS_3 \cdot P \cdot D$ complexes (gray bars) formed using the "CG_5C", "AG_5A", and "TG_5T" versions of the L oligonucleotide (and the corresponding cL, P, and D strands). Lower: The black (L·cL duplexes) and gray histograms ($LS_3 \cdot P \cdot D$ complexes) describe the ratios of damage at their 5′-most distal guanines (GGd in panel A) relative to the 5′-most proximal guanines (GGp in panel A). The white bars plot the ratio of the gray bars to the corresponding black bars, as percentage values.

to a number of the earlier studies on antiparallel quadruplexes (*30*−*32*).

Our charge transfer experiments were carried out six independent times, and the key features of the data observed were reproducible. Figure 5B shows two histograms, the first of which plots levels of charge-flow-related DNA cleavage at the 5′-most G of the distal guanine doublet ("GGd" in Figure 5A) of the three L·cL duplexes (black bars) compared to the three $LS_3 \cdot P \cdot D$ complexes (gray bars) formed using the "CG_5C", "AG_5A", and "TG_5T" versions of the L oligonucleotide (and their corresponding cL, P, and D strands). A comparison of damage at the distal guanine, "GGd", as a percentage of the overall damage within a given L oligomer, provides a useful indicator of the effectiveness of charge flow from the anthraquinone across the proximal duplex and across the D-Q-D construct. The histogram shows that, in all instances, less charge reaches GGd in the $LS_3 \cdot P \cdot D$ complexes relative to the GGd in the analogous L·cL complexes (although the "AG_5A"-based $LS_3 \cdot P \cdot D$ complex is a notably better conductor than the other two).

The consistently smaller numbers for guanine damage over the length of each $LS_3 \cdot P \cdot D$ complex relative to its duplex equivalent (even in a comparison of the relatively similarly behaving AG_5A duplex and $LS_3 \cdot P \cdot D$ complexes, the guanine damage level is at $7.4 \pm 3.3\%$ of the total guanines in the duplex versus $3.0 \pm 0.9\%$ in $LS_3 \cdot P \cdot D$) raise interesting questions about the "protective" value of the G-quadruplex. In all of the duplex and D-Q-D constructs, the DNA sequence in the immediate vicinity of the anthraquinone moiety is identical (the AQ stacks on a duplex that is invariant in sequence for 14 base pairs). It is therefore reasonable to postulate that the efficiency of charge injection by the photoirradiated AQ into its proximal DNA base stack is comparable for all of the constructs. Guanine oxidation occurs via reaction of guanine radical cations with water or oxygen, and a number of the oxidized guanine products are susceptible to cleavage by hot piperidine. The significantly higher levels of damage seen in duplexes relative to the D-Q-D complexes suggest that the 20 guanine bases that make up the quadruplex act as a significant and protective reservoir against guanine oxidation relative to the 5 central and contiguous guanines present as G-C base pairs in the duplex. It may be that a guanine radical cation localized in the parallel quadruplex does not react easily with either oxygen or water (with the notable exception, again, of the 5′-most guanine of the quadruplex in the AG_5A D-Q-D complex); alternatively, guanine oxidation products formed in the quadruplex may be resistant to cleavage by hot piperidine (*42*). Further work will be needed to investigate this last possibility.

The data shown in Figure 5 testify further to the ability of electron holes to flow from a duplex into a quadruplex and out again into a second duplex. The question of the relative attenuation provided by the block of five G-quadruplexes relative to five G-C base pairs can be assessed by comparing the ratio of damage at the distal guanine doublet in a given construct with damage at the proximal guanine doublet. This parameter is plotted in the lower histogram of Figure 5B. The black (L·cL duplexes) and

gray histograms ($LS_3 \cdot P \cdot D$ complexes) describe the ratios of damage at their 5′-most distal guanines (GGd in Figure 5A) relative to the 5′-most proximal guanines (GGp in Figure 5A). In all cases, the duplex gives a higher ratio of distal to proximal guanine damage relative to the D-Q-D construct (the AG_5A-based constructs are the best conductors in each class). The white bars in the lower histogram plot the ratio of the gray bars (distal/proximal ratio in D-Q-D) to the corresponding black bars (distal/proximal ratio in duplexes). A remarkably constant number (~50%) is calculated for each of duplex/D-Q-D combinations. In other words, a parallel DNA quadruplex appears to be approximately half as conductive of electron holes as a comparable length of G-C base pair-containing duplex.

The three sets of D-Q-D complexes, while essentially similar to each other in terms of their overall conduction and guanine damage properties, nevertheless show some key and reproducible differences. Most notable are (a) the better overall conductivity as well as (b) rare oxidative damage observed in a quadruplex-forming guanine within the $LS_3 \cdot P \cdot D$ complex formed using the "AG_5A" L oligomer. The distinctness of these properties from those of the $LS_3 \cdot P \cdot D$ complexes formed by the other L oligomers suggests that the specific geometry and dynamics of individual duplex−quadruplex junctions as well as the identity of the base pair(s) at the junction do impact on both the efficiency of charge flow between the two helical forms and any oxidative protection afforded to guanines within a quadruplex.

One small comment is appropriate here to our observation that in our L·cL duplex (and, to a lesser extent, in $LS_3 \cdot P \cdot D$) damage to GGd is consistently higher than to GGp. A number of other studies (*19*, *21*, *44*), which have also used AQ as photooxidant, have found a GGp > GGd pattern from their particular duplexes. We, however, find a reproducible GGd > GGp pattern from a number of duplexes under study in our laboratory. The GGd > GGp pattern is replicated at different doses of AQ irradiation (all within the linear range of response) as well as at different temperatures (0−37 °C). The pattern is, moreover, not an artifact of the location of the ^{32}P label distally to the AQ label. Placing the two labels side by side (via 3′-^{32}P labeling) gives the same GGd > GGp result (unpublished data). The variation in observation by the different groups may lie in the specifics of the local sequences surrounding the GGd and GGp guanines in the different duplexes and in differences in local thermodynamic minima as well as, conceivably, in differences of back charge transfer efficiencies from the GGp base to AQ. We are currently actively investigating this overall phenomenon.

The above charge-flow experiments were carried out at 4° C in the presence of 100 mM KCl and 1 mM $MgCl_2$. We speculated whether a higher concentration of magnesium in the irradiation buffer might help to stabilize the duplex−quadruplex junctions and so modify the conductivity and guanine damage patterns for the "AG_5A" D-Q-D construct. Figure 6 shows data on charge conduction-generated guanine damage and DNA cleavage in the presence of 1 and 5 mM magnesium, respectively. It can be seen that the overall levels of guanine damage are lower in the presence of higher magnesium, possibly connected to slower DNA dynamics (which are important for the conduction mechanism of DNA) at the higher magnesium concentration. However, the overall patterns of conduction are not substantially different under the two conditions, and the 5′-most quadruplex-forming guanine in the L strand continues to suffer oxidative damage under the two conditions.

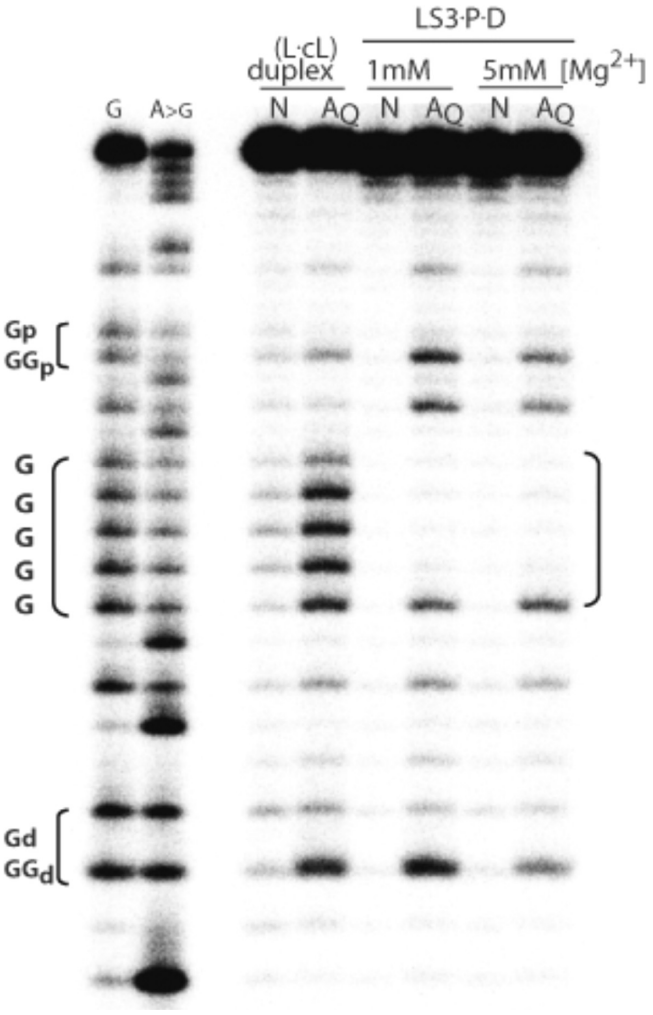

FIGURE 6: Levels of charge-flow-related DNA cleavage in the $LS_3 \cdot P \cdot D$ complexes (where L is "AG_5A") as a function of magnesium concentration. The duplex sample, shown for comparison, was irradiated in the presence of 1 mM Mg^{2+}.

In order to get a clear idea about what specific structural features of $LS_3 \cdot P \cdot D$ give rise to the charge conduction and guanine damage properties described above, it was necessary to investigate the properties of a number of control constructs (shown schematically in Figure 3), which vary from $LS_3 \cdot P \cdot D$ in specific ways. Figure 7 shows the data for charge conduction-generated guanine damage/DNA cleavage for the $LS_3 \cdot P$, $L \cdot P \cdot D$, Gap 3, and Gap5 constructs, in addition to the standards, $LS_3 \cdot P \cdot D$ and L·cL (in all of these constructs, the identity of L is "AG_5A"). In the $LS_3 \cdot P$ construct, little damage was expected in the distal doublets relative to L·cL or $LS_3 \cdot P \cdot D$ given that the $LS_3 \cdot P$ construct lacks the distal D-arm. However, some damage in that distal, single-stranded stretch of L within $LS_3 \cdot P$ is seen. There are precedents for this low level of charge conduction through single-stranded DNA containing multiple stretches of guanine, and charge transfer is thought to be mediated by transient foldbacks and G-G base pair formation by the single-stranded portion (*45*, *48*). By contrast, none of the constructs, Gap3, Gap5, or $L \cdot P \cdot D$, show any detectable cleavage at GGd, emphasizing strongly that the formation of the distal (as well as proximal) duplex−quadruplex junction is essential for efficient charge flow through a D-Q-D composite. In terms of guanine damage within the quadruplex, interestingly, none of $LS_3 \cdot P$, Gap3, and Gap5 (which all contain quadruplexes) show any level

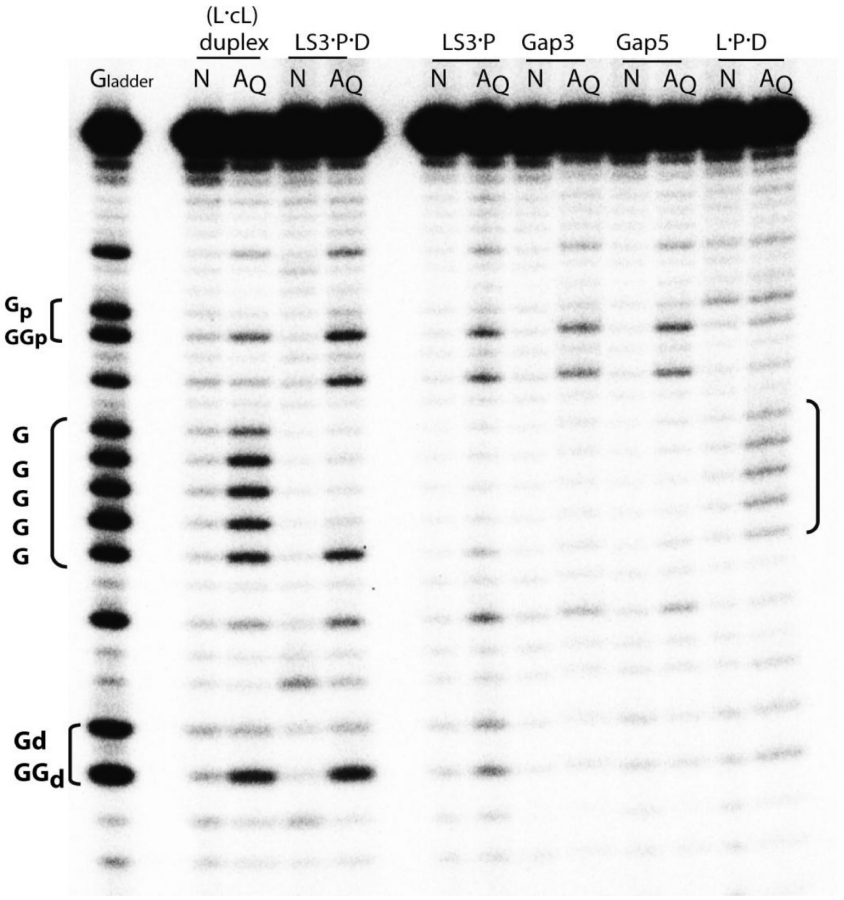

FIGURE 7: Comparison of the charge-flow characteristics of a number of control DNA constructs (schematized in Figure 3) relative to the L·cL and $LS_3 \cdot P \cdot D$ complexes.

of cleavage of the quadruplex guanines, unlike the striking cleavage of the 5′-most quadruplex guanine in $LS_3 \cdot P \cdot D$. The oxidizability of the latter then clearly has to do with the structural and/or dynamic details of the distal quadruplex−duplex junction of $LS_3 \cdot P \cdot D$ formed using the "AG_5A" oligomer. Interestingly, in the L·P·D construct, which consists of two duplexes linked by a single-stranded DNA stretch of dG_5, the five single-stranded guanines do suffer a very low level of damage, possibly from traces of singlet oxygen generated from the irradiation of AQ (*25*). Here, as has been noted before, enhanced damage is not seen at the 5′-end of the guanine stretch (*45*), as it is seen in duplexes.

DISCUSSION

In this paper we have studied the charge conduction properties of a parallel, four-stranded quadruplex. Intermolecular parallel quadruplexes were first proposed to be involved in the alignment of homologous choromosomes at meiosis (*7*). More recently, even intramolecular folds of telomeric and other genomic G-rich DNA sequences have been proposed, in a number of cases, to form parallel-stranded quadruplexes. A notable case is the human telomeric repeat, which was shown in a high-resolution crystal structure to be parallel-stranded (*35*). Subsequent studies on the human telomeric repeat in solution have found its quadruplex fold to be highly polymorphic, raising doubts on the biological relevance of the wholly parallel structure determined by crystallography (*36*−*40*). However, a recent study on the fold of human telomeric repeats under conditions of molecular crowding, such as may be found *in vivo*, has reiterated the possible relevance of the all-parallel fold (*41*−*49*).

Key questions we asked in this study are as follows: (a) Can charge transit into a parallel quadruplex from a duplex and vice versa? (b) To what extent do the specifics of duplex−quadruplex junctions matter? (c) Does a parallel-stranded quadruplex constitute a charge sink for electron holes, relative to duplexes and to antiparallel quadruplexes? (d) Does existing within a parallel quadruplex offer protection from oxidative damage to guanines (again, relative to duplexes and antiparallel quadruplexes)? The answer to all of the above appears to be "yes". In substantial agreement with prior studies on antiparallel quadruplexes (*31*, *32*, *34*), charge appears to be able to transit freely between duplex and quadruplex. The precise identity of bases at duplex−quadruplex junctions does seem to matter, although we do not find this to be a large effect. Overall levels of G-damage within our three D-Q-D constructs is significantly less than in their corresponding duplex controls; hence, the quadruplexes appear to be acting as charge sinks. However, with regard to guanine damage within the parallel quadruplex itself, our most interesting finding is the almost negligible damage (with a single exception) to such guanines. This high level of oxidative protection is strikingly different from much of the prior literature on antiparallel duplexes (*30*−*33*); for example, in Delaney and Barton's (*31*) and Ndlebe and Schuster's (*32*) studies, which utilized different duplex/quadruplex conjugates of complex secondary structure, preferential oxidative damage of quadruplex guanines was observed.

What causes might underlie the differences in charge conduction behavior noted between parallel and antiparallel quadruplexes? Three levels of difference might be considered

a priori: structural, electronic/thermodynamic, and differences in reaction with water. First, our D-Q-D constructs were designed to optimize both base stacking and concomitant charge flow between duplex and quadruplex elements. In general, the earlier studies on antiparallel quadruplex/duplex composites did not especially ensure this. In terms of electronic properties and thermodynamic sinks for electron holes, it should be noted that a parallel quadruplex is made up of deoxyguanosines with obligatory *anti*-glycosidic orientations, whereas antiparallel quadruplexes necessarily harbor *both anti* and *syn* conformations. This key divergence leads to differences, in the way that successive G-quartets overlap with each other in the two gross kinds of quadruplexes (*50*−*52*). As has been noted before, the specific geometry of overlap has tremendous consequence for the oxidizability of contingous guanines within *duplexes* (*17*−*19*). Analogously, the differences in "sink" behavior between antiparallel and parallel quadruplexes may be similarly rooted in the specific, and different, structures of their base stacks.

The "observable" guanine damage in our data reflects levels of reaction that individual guanine radical cations undergo with water/oxygen. Within a uniform duplex, water reaction rates are typically much slower than charge-flow rates; thus, the G-damage pattern is a "snapshot" of the equilibrium distribution of G radical cations along the double helix (*17*−*19*). In complex duplex−quadruplex composites, however, the uniformity and slowness of the water reaction rates cannot be assumed. Guanines highly exposed to the solvent would be expected to react efficiently with water (*25*, *53*), over and above the kinetics of charge flow to and away from them. Many of the antiparallel quadruplexes studied in earlier studies had built-in "terminal" quadruplexes (*31*, *32*, *34*), with terminal quartets exposed directly to the solvent. In our D-Q-D complexes, however, the quadruplex is sandwiched between two duplexes, with helical stress minimized at the junctions. The far lower quadruplex G-damage patterns seen in our experiments, relative to earlier studies, may be related to these factors. In addition, it has to be noted that the groove structures of parallel quadruplexes, on one hand, and part or wholly antiparallel quadruplexes, on the other, are often strikingly different, leading to differences in hydration and, possibly, to efficiency of the water reaction. A final structural difference with possible consequence to charge conduction properties is the absence of single-strand loops in our D-Q-D structures, whereas the earlier antiparallel structures necessarily had built-in foldback loops, with unpredictable influences on both the charge-flow and water reaction properties of those quadruplexes.

In summary, we postulate that it is not so much the formation of the quadruplex itself that dictates where charge-flow-related oxidation occurs; rather, it is the specifics of the structure (including the solvent accessibility of the specific grooves formed) and sequence context of the folded quadruplex that dictate the preferred sites of oxidative damage. Overall, our results lend credence to the hypothesis that, *in vivo*, telomeric guanine repeats may act as sinks to draw away oxidative damage from more critical regions of the genome. If such telomeric guanines were to be present as quadruplexes, oxidative damage to them would likely vary depending on the specific characteristics of the quadruplexes formed.

From a different perspective, given the demonstration here that electron holes can pass through stacked duplex−quadruplex junctions, it will be interesting to electrochemically explore the charge carrier properties of D-Q-D constructs arranged in monolayers upon a gold electrode. Indeed, such experimentation is currently under way in our laboratories. Our results here also raise the possibility that parallel G-quadruplexes might find a role or roles in the design of DNA-based biosensors (for instance, refs (*27*−*29*)) and of DNA-based nanocircuitry, where a G-quadruplex might function as a junction or conductive node for duplexes serving as DNA nanowires. Preliminary results from our laboratory give a positive indication in this regard.

ACKNOWLEDGMENT

We are grateful to Dr. Melanie O'Neill and to group members of the Sen and the Yu laboratories for helpful discussions. We thank Gurpreet Sekhon for contribution of the table of contents figure.

REFERENCES

1. Wellinger, R., and Sen, D. (1997) The DNA structures at the ends of eukaryotic chromosomes. *Eur. J. Cancer 33*, 735–749.
2. Mirkin, S. M. (2008) Discovery of alternative DNA structures: a heroic decade (1979−1989). *Front. Biosci. 13*, 1064–1071.
3. Watson, J. D. (1972) Origin of concatemeric T7 DNA. *Nat. New. Biol. 239*, 197–201.
4. Greider, C. W., and Blackburn, E. H. (1985) Identification of a specific telomere terminal transferase activity in *Tetrahymena* extracts. *Cell 43*, 405–413.
5. Grunstein, M. (1997) Molecular model for telomeric heterochromatin in yeast. *Curr. Opin. Cell Biol. 9*, 383–387.
6. Brunet, A. (2007) Aging and cancer: killing two birds with one worm. *Nat. Genet. 39*, 1306–1307.
7. Sen, D., and Gilbert, W. (1988) Formation of parallel four-stranded complexes by guanine-rich motifs in DNA and its implications for meiosis. *Nature 334*, 364–366.
8. Williamson, J. R., Raghuraman, M. K., and Cech, T. R. (1989) Monovalent cation-induced structure of telomeric DNA: the G-quartet model. *Cell 59*, 871–880.
9. Sundquist, W. I., and Klug, A. (1989) Telomeric DNA dimerizes by formation of guanine tetrads between hairpin loops. *Nature 342*, 825–829.
10. Sen, D., and Gilbert, W. (1990) A sodium-potassium switch in the formation of four-stranded G4-DNA. *Nature 344*, 410–414.
11. Sen, D., and Gilbert, W. (1992) Novel DNA superstructures formed by telomere-like oligomers. *Biochemistry 31*, 65–70.
12. Nunez, M., Hall, D. B., and Barton, J. K. (1999) Long-range oxidative damage to DNA: effects of distance and sequence. *Chem. Biol. 6*, 85–97.
13. Friedman, K. A., and Heller, A. (2001) On the non-uniform distribution of guanine in introns of human genes: possible protection of exons against oxidation by proximal intron poly-G sequences. *J. Phys. Chem. B 105*, 11858–11865.
14. Heller, A. (2000) On the hypothesis of cathodic protection of genes. *Faraday Discuss. 116*, 1–13.
15. Friedman, K. A., and Heller, A. (2004) Guanosine distribution and oxidation resistance in eight eukaryotic genomes. *J. Am. Chem. Soc. 126*, 2368–2371.
16. Eley, D. D., and Spivey, D. I. (1962) The semiconductivity of organic substances, Part 9—nucleic acid in the dry state. *Trans. Faraday Soc. 58*, 411–415.
17. Turro, N., and Barton, J. K. (1998) Paradigms, supermolecules, electron transfer and chemistry at a distance. What's the problem? The science or the paradigm?. *J. Biol. Inorg. Chem. 3*, 201–209.
18. Giese, B. (2002) Electron transfer in DNA. *Annu. Rev. Biochem. 71*, 51–70.
19. Schuster, G. B. (2000) Long-range charge transfer in DNA: transient structural distortions control the distance dependence. *Acc. Chem. Res. 33*, 253–260.
20. Henderson, P. T., Jones, D., Hampikian, G., Kan, Y., and Schuster, G. B. (1999) Long-distance charge transport in duplex DNA: the phonon-assisted polaron-like hopping mechanism. *Proc. Natl. Acad. Sci. U.S.A. 96*, 8353–8358.
21. Joy, A., and Schuster, G. B. (2005) Long-range radical cation migration in DNA: investigation of the mechanism. *Chem. Commun. 22*, 2778–2784.
22. Meggers, E., Michel-Beyerle, M. E., and Giese, B. (1998) Sequence dependent hole transfer in DNA. *J. Am. Chem. Soc. 120*, 12950–12955.

23. Ratner, M. (1999) Electronic motion in DNA. *Nature 397*, 480–481.
24. Jortner, J., Bixon, M., Langenbacher, T., and Michel-Beyerle, M. E. (1998) Charge transfer and transport in DNA. *Proc. Natl. Acad. Sci. U.S.A. 95*, 12759–12765.
25. Burrows, C. J., and Muller, J. G. (1998) Oxidative nucleobase modifications leading to strand scission. *Chem. Rev. 98*, 1109–1151.
26. Odom, D. T., and Barton, J. K. (2001) Long-range oxidative damage in DNA/RNA duplexes. *Biochemistry 40*, 8727–8737.
27. Fahlman, R. P., and Sen, D. (2002) DNA conformational switches as sensitive electronic sensors of analytes. *J. Am. Chem. Soc. 124*, 4610–4616.
28. Sankar, C. G., and Sen, D. (2004) DNA helix-stack switching as the basis for the design of versatile deoxyribosensors. *J. Mol. Biol. 340*, 459–467.
29. Huang, Y. C., Ge, B., Sen, D., and Yu, H. Z. (2008) Immobilized DNA switches as electronic sensors for picomolar detection of plasma proteins. *J. Am. Chem. Soc. 130*, 8023–8029.
30. Szalai, V. A., and Thorp, H. H. (2000) Electron transfer in tetrads: adjacent guanines are not hole traps in G quartets. *J. Am. Chem. Soc. 122*, 4524–4525.
31. Delaney, S., and Barton, J. K. (2003) Charge transport in DNA duplex/quadruplex conjugates. *Biochemistry 42*, 14159–14165.
32. Ndlebe, T., and Schuster, G. B. (2006) Long-distance radical cation transport in DNA: Horizontal charge hopping in a dimeric quadruplex. *Org. Biomol. Chem. 4*, 4015–4021.
33. Kawai, K., Fujitsuka, M., and Majima, T. (2005) Selective guanine oxidation by UVB-irradiation in telomeric DNA. *Chem. Commun.,* 1476–1477.
34. Pothukuchy, A., Mazzitelli, C. L., Rodriguez, M. L., Tuesuwan, B., Salazar, M., Brodbelt, J. S., and Kerwin, S. M. (2005) Duplex and quadruplex DNA binding and photocleavage by trioxatriangulenium ion. *Biochemistry 44*, 2163–2172.
35. Parkinson, G. N., Lee, M. P., and Neidle, S. (2002) Crystal structure of parallel quadruplexes from human telomeric DNA. *Nature 417*, 876–880.
36. Dai, J., Carver, M., and Yang, D. (2008) Polymorphism of human telomeric quadruplex structures. *Biochimie 90*, 1172–1183.
37. Petraccone, L., Trent, J. O., and Chaires, J. B. (2008) The tail of the telomere. *J. Am. Chem. Soc. 130*, 16530–16532.
38. Li, J., Correia, J. J., Wang, L., Trent, J. O., and Chaires, J. B. (2005) Not so crystal clear: the structure of the human telomere G-quadruplex in solution differs from that present in a crystal. *Nucleic Acids Res. 33*, 4649–4659.
39. Ambrus, A., Chen, D., Dai, J., Bialis, T., Jones, R. A., and Yang, D. (2006) Human telomeric sequence forms a hybrid-type intramolecular G-quadruplex structure with mixed parallel/antiparallel strands in potassium solution. *Nucleic Acids Res. 34l*, 2723–2735.
40. Xu, Y., Noguchi, Y., and Sugiyama, H. (2006) The new models of the human telomere d[AGGG(TTAGGG)$_3$] in K^+ solution. *Bioorg. Med. Chem. 14*, 5584–5591.
41. Xue, Y., Kan, Z. Y., Wang, Q., Yao, Y., Liu, J., Hao, Y. H., and Tan, Z. (2007) Human telomeric DNA forms parallel-stranded intramolecular G-quadruplex in K^+ solution under molecular crowding condition. *J. Am. Chem. Soc. 129*, 11185–11891.
42. Aboul-ela, F., Murchie, A. I. H., and Lilley, D. M. J. (1992) NMR study of parallel-stranded tetraplex formation by the hexadeoxynucleotide d(TG$_4$T). *Nature 360*, 280–282.
43. Laughlan, G., Murchie, A. I. H., Norman, D. G., Moore, M. H., Moody, P. C., Lilley, D. M. J., and Luisi, B. (1994) The high-resolution crystal structure of a parallel-stranded guanine tetraplex. *Science 265*, 520–524.
44. Williamson, J. R. (1994) G-quartet structures in telomeric DNA. *Annu. Rev. Biophys. Biomol. Struct. 23*, 703–730.
45. Bergeron, L. J., Sen, K., and Sen, D. (2008) A guanine-linked end-effect is a sensitive reporter of charge flow through DNA and RNA double helices. *Biochimie 90*, 1064–1073.
46. Maxam, A. M., and Gilbert, W. (1980) Sequencing end-labeled DNA with base-specific chemical cleavages. *Methods Enzymol. 65*, 499–560.
47. Williams, T., Dohno, C., Stemp, E. D. A., and Barton, J. K. (2004) Effects of the photooxidant on DNA-mediated charge transport. *J. Am. Chem. Soc. 126*, 8148–8158.
48. Kan, Y., and Schuster, G. B. (1999) Long-range guanine damage in single-stranded DNA: charge transport through a duplex bridge and in a single-stranded overhang. *J. Am. Chem. Soc. 121*, 10857–10864.
49. Karimata, H., Miyoshi, D., and Sugimoto, N. (2005) Structure and stability of DNA quadruplexes under molecular crowding conditions. *Nucleic Acids Symp. Ser. (Oxford) 49*, 239–240.
50. Burge, S., Parkinson, G. N., Hazel, P., Todd, A. K., and Neidle, S. (2006) Quadruplex DNA: sequence, topology and structure. *Nucleic Acids Res. 34*, 5402–5415.
51. Patel, D. J., Phan, A. T., and Kuryavyi, V. (2007) Human telomere, oncogenic promoter and 5′-UTR G-quadruplexes: diverse higher order DNA and RNA targets for cancer therapeutics. *Nucleic Acids Res. 35*, 7429–7455.
52. Huppert, J. L. (2008) Four-stranded nucleic acids: structure, function and targeting of G-quadruplexes. *Chem. Soc. Rev. 37*, 1375–1384.
53. Leung, E. K. Y., and Sen, D. (2007) Electron hole flow patterns through the RNA-cleaving 8-17 deoxyribozyme yield unusual information about its structure and folding. *Chem. Biol. 14*, 41.